Multivalent ion driven condensation of DNA-actin polyelectrolyte mixtures

Olena V. Zribi[1], Hee Kyung[1], Ramin Golestanian[2,3], Tanniemola B. Liverpool[2,4] and Gerard C. L. Wong[1](*)

[1] *Department of Materials Science & Engineering, Department of Physics, Department of Bioengineering, University of Illinois at Urbana-Champaign, IL 61801, USA*
[2] *Isaac Newton Institute for Mathematical Sciences, Cambridge, CB3 0EH, UK*
[3] *Institute for Advanced Studies in Basic Sciences, Zanjan 45195-159, Iran*
[4] *Department of Applied Mathematics, University of Leeds, Leeds LS2 9JT, UK*

PACS. 82.35.Rs – Polyelectrolytes.
PACS. 82.35.Pq – Biopolymers, biopolymerization.
PACS. 87.15.AA – Theory and modeling; computer simulation.

Abstract. – Multivalent ions can induce condensation of like-charged polyelectrolytes into compact states, a process that requires different ion valence for different polyelectrolyte species. We have examined the trivalent ion induced condensation behavior in binary anionic polyelectrolyte mixtures consisting of DNA coils and F-actin rods, and observe a micro-phase separation between the two polyelectrolytes into coexisting finite-sized F-actin bundles and DNA toroids. Further, by increasing the DNA volume fraction in the mixture, condensed F-actin bundles can be completely destabilized, leading to only DNA condensation within the mixture. We examine a number of possible causes and propose a model based on polyelectrolyte competition for ions.

Electrostatics in complex fluids often exhibits counterintuitive effects [1]. Multivalent ions can mediate attraction between like-charged polyelectrolytes in aqueous solution and induce condensation into compact states, in contradiction to all mean field theories [2–7]. Recent experimental examples include DNA, F-actin, microtubules, and filamentous viruses [8]. It is also known that ions of different valences are generally required to condense different polyelectrolytes. Trivalent ions are usually required to condense DNA, while only divalent ions are required to condense F-actin and viruses of the Ff family, and monovalent ions do not condense any of them [9]. What happens when multivalent ions of a given valence are used to condense a mixture of two different polyelectrolytes? This represents a broad class of problems with many combinations. Individual polyelectrolyte parameters, such as charge density, contour length, and flexibility, can be varied, and the ion valence can be chosen to condense either or both of the polyelectrolytes in the mixture. The organization of the polyelectrolyte mixture can have a wide range of structural possibilities, from ordered or disordered composite states to complete phase separation. The phase behavior of these mixed polyelectrolyte systems with multivalent ions has applications ranging from water purification to cystic fibrosis.

(*) E-mail: gclwong@uiuc.edu

Here, we examine the condensation behavior in binary anionic biological polyelectrolyte mixtures consisting of highly-charged DNA coils and F-actin rods in the presence of spermidine, a trivalent cation capable of condensing both polyelectrolyte species in isolation. Using synchrotron small angle x-ray scattering (SAXS) and laser-scanning confocal microscopy, we find that the system undergoes a micro-phase separation into coexisting finite-sized, close-packed F-actin bundles and close-packed DNA toroids that can mutually adhere and assemble into large complexes, rather than collapse into a homogeneous composite DNA-actin condensate. Further, by increasing the DNA volume fraction in the mixture, condensed F-actin bundles can be completely destabilized, leading to only DNA condensation within the mixture. We examine a number of possible causes for this behavior and propose a simple model based on polyelectrolyte competition for ions.

Both DNA (diameter $D_{\rm DNA}\sim$2.0 nm, charge density $\lambda_{\rm DNA}\sim -e/0.17$ nm, persistence length $\xi_{\rm DNA}\sim$50 nm) and F-actin (diameter $D_{\rm Actin}\sim$7.5 nm, charge density $\lambda_{\rm Actin}\sim -e/0.25$ nm at pH 7, persistence length $\xi_{\rm Actin}\sim$10 μm) have linear charge densities larger than the Manning criterion [2,10] for counterion condensation. F-actin is larger in diameter and stiffer than DNA, but has a lower charge density. Mixtures of DNA and actin in the presence of multivalent salts are particularly interesting since both polyelectrolytes are found at high concentrations ($\sim$1–10 mg/ml) in the mucus layer lining the airways of cystic fibrosis (CF) patients [11]. Moreover, polycationic small molecule antibiotics such as the aminoglycosides (e.g. tobramycin) are commonly used for CF treatment, and can lead to drastic changes in the phase behavior of the DNA-actin mixture in the airways. A study of the DNA-actin-spermidine model system may help elucidate the complex biophysical interactions between different components in the CF airway.

Monomeric actin (G-actin) (molecular weight, 43000) was prepared from a lyophilized powder of rabbit skeletal muscle purchased from Cytoskeleton (Denver). The nonpolymerizing G-actin solution contained a 5 mM Tris buffer at pH 8.0, with 0.2 mM $CaCl_2$, 0.5 mM ATP, 0.2 mM DTT, and 0.01% NaN_3. G-actin (2 mg/ml) was polymerized into F-actin with the addition of salt (100 mM KCl final concentration). Samples were typically polymerized for 1 hour. Human plasma gelsolin, an actin severing and capping protein (Cytoskeleton.com), was used to regulate the F-actin length. The average length of F-actin is controlled by the gelsolin concentration, which has been independently calibrated. The filaments were treated with phalloidin (molecular weight 789.2) to prevent actin depolymerization. F-actin gels were ultracentrifuged at $100000 \times g$ for 1 hour to pellet the filaments. After the removal of the supernatant buffer solution, the F-actin was resuspended in Millipore H_2O (18.2 MΩ) to the desired concentration. Lambda phage DNA (New England Biolabs, Inc.) was ethanol-precipitated and resuspended in deionized Millipore water (18 MΩ). Spermidine trihydrochloride (MW=254.6; Sigma-Aldrich) is dissolved to generate trivalent ions (H_3N^+-CH_2-CH_2-CH_2-CH_2-N^+H_2-CH_2-CH_2-CH_2-N^+H_3) in solution. Mixtures of F-actin, λ-DNA and salt solutions were combined, thoroughly mixed and sealed in the quartz capillaries for x-ray studies.

For the confocal microscopy experiments, F-actin was dyed using Alexa Fluor 488 phalloidin (Molecular Probes) at a 1:1 monomer molar ratio, and the DNA was dyed with POPO-3 (Molecular Probes) at a concentration of one dye molecule per 10 base pairs. Typical sample concentrations were $\sim$0.03 mg/ml for actin and $\sim$0.02 mg/ml for DNA. The samples were imaged using a Leica TCS SP2 confocal microscope equipped with 63$\times$ oil immersion objective.

Small angle x-ray scattering (SAXS) measurements were performed using both an in-house x-ray source as well as beam line 4-2 and 34ID-C at the Stanford Synchrotron Radiation Laboratory (SSRL) and Advanced Photon Source (APS). For the in-house experiments, incident CuKα radiation ($\lambda = 1.54$ Å) from a Rigaku rotating-anode generator was monochromatized and focused using Osmic confocal multilayer optics, and scattered radiation was collected on

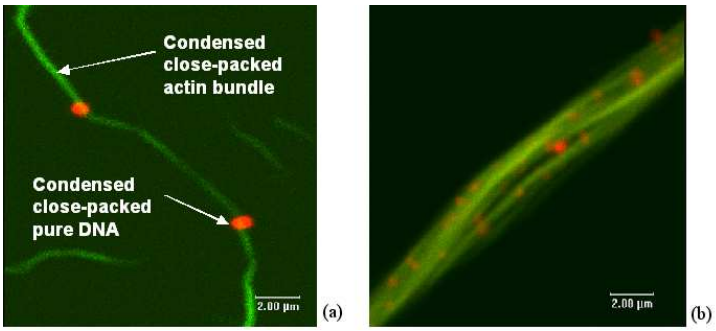

Fig. 1 – Structure of actin/DNA/Spermidine^{3+} condensates from confocal microscopy: F-actin (10 μm average length) was dyed with Alexa Fluor 488 (green), λ-DNA (16 μm length) was dyed with POPO-3 (red). (a) Close-packed DNA globules (presumably toroids) adhere to close-packed actin bundles. These structures can in turn organize into larger composite bundles (b). The spermidine^{3+} concentration is 10 mM, which is sufficiently high to condense both species. The molar ratio between DNA base pairs and monomeric G-actin is D/A = 15. Global concentration of actin is 0.03 mg/ml, DNA 0.023 mg/ml.

a Bruker 2D wire detector (pixel size = 105 μm). For the SSRL BL-4-2 experiments, incident x-rays were monochromatized to 10 keV using a double-bounce Si(111) crystal, and focused using a cylindrical mirror, with a beam size of 300×300 μm^2. The scattered radiation was collected using a MAR Research charged-coupled device camera (pixel size = 79 μm). For the APS experiments, incident x-rays were monochromatized to 9 keV using a double-bounce Si(111) reflection, with final beam size of 400×400 μm^2. The scattered radiation was collected using a Roper Scientific direct-detection CCD camera (pixel size = 20 μm). The 2D SAXS data from all setups have been checked for mutual consistency.

Mixed DNA-actin condensates have a number of possible structures. The diameters of F-actin and DNA are such that it is possible to intercalate DNA strands in the interstices of a close-packed columnar hexagonal actin lattice. Confocal microscopy was used to investigate the large-scale organization of DNA-actin condensates in the dilute regime (∼0.01 mg/ml for both actin and DNA concentrations). Instead of a global phase separation or a composite condensate, the DNA-actin system undergoes a micro-phase separation into coexisting finite-sized F-actin bundles (green) and DNA globules (red), presumably the fluorescence signature of the generic toroidal structures observed for condensed DNA, details of which cannot be resolved by optical microscopy (Fig. 1a). These bundles and globules have typical diameters in the sub-micron range [12] (microscope point spread function ∼0.25 μm). Moreover, these objects can mutually adhere to one another and assemble into composite aggregates consisting of large numbers of actin bundles and DNA globules (Fig. 1b). Attractive interactions such as van der Waals attractions and electrostatic correlations in strongly bound spermidine ions between the toroids and bundles can potentially contribute to this composite actin-DNA organization. In the context of the current debate on the physical origin of observed condensed polyelectrolyte bundle sizes [13–15], it is interesting to note that actin bundles preferentially adhere to DNA globules or weakly aggregate into a nematic network with other actin bundles rather than form close-packed bundles of larger radii from individual actin filaments. Moreover, we do not observe evolution of these aggregates into larger radii bundles (within ∼24 hours). These observations suggest a thermodynamic limit to the bundle size, although more work will be necessary in order to elucidate the interactions between the DNA and actin condensates. For

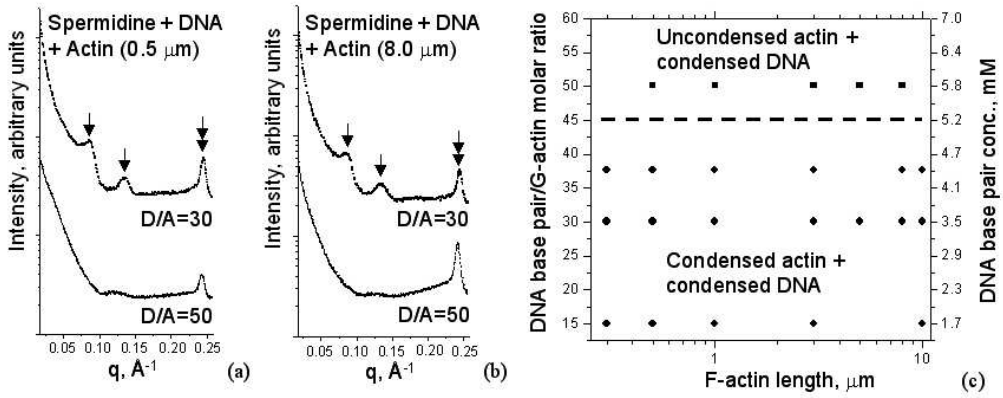

Fig. 2 – There are two regimes of behavior for actin-DNA mixtures condensed by trivalent salts (Spermidine^{3+}). At low D/A ratios, both actin and DNA are condensed. At high D/A ratios, only DNA is condensed. (a) Typical SAXS data for samples containing short F-actin (average length 0.5 μm) at 5 mg/ml, λ-DNA at 2.28 mg/ml to 3.8 mg/ml, and Spermidine^{3+} at 5 mM. Diffraction peaks at 0.086 and 0.136 Å^{-1} correspond to the bundled phase of F-actin. The peak at 0.245 Å^{-1} corresponds to close-packed DNA. (b) Similar behavior is observed for long F-actin (average length 8 μm) under the same conditions. (c) Phase diagram section for actin/DNA/Spermidine^{3+} system at 5 mM Spermidine concentration that is sufficiently high to condense both species. The actin concentration is held constant at 5 mg/ml actin, while the DNA concentration is varied.

example, it is possible that DNA toroids preferentially adhere to bundles rather than to other toroids due to the reduced surface curvature. It is clear from these experiments, however, that the DNA and actin do not pack together into a homogeneous composite structure within these condensates.

The microscopic organization of these DNA-actin condensates can be seen in a series of synchrotron SAXS experiments (Fig. 2a-b) for samples at different DNA base pair to actin monomer molar ratios (D/A). The DNA concentration was varied between 1.14 and 3.8 mg/ml for constant actin and spermidine^{3+} concentrations (5mg/ml and 5mM respectively). This corresponds to 116 μM concentration of actin monomers and 1.7–5.8 mM concentration of DNA base pairs. Fig 2a shows a sample at a D/A=30. Two sets of diffraction peaks can be observed, corresponding to F-actin correlations within the bundles (single arrow, inter-actin spacing = 73 Å) and DNA correlations in the globules (double arrow, inter-DNA spacing = 25 Å). These distances are close to the hard-rod diameters of these biopolymers indicate that they are closely packed. We speculate that it is the surface charge density mismatch between the DNA and F-actin that drives this microphase separation into pure actin bundles and pure DNA globules. In this context, it would be interesting to see what happens to mixtures of DNA with polyelectrolytes that have a similar diameter to actin but at charge densities that can closely match with DNA.

As the molar ratio between DNA and actin is increased (higher D/A ratio), we observe a de-condensation of actin, so that only DNA is condensed within the DNA-actin mixture. Figure 2a shows that as D/A is increased from 30 to 50, the diffraction peaks that correspond to actin packing within the bundles (at q = 0.086 Å^{-1} and q = 0.136 Å^{-1}) disappear, leaving only the DNA close-packing peak at q = 0.25 Å^{-1}. This is surprising since 5 mM spermidine^{3+}

is sufficient to condense either species in isolation (which has been independently confirmed). This phenomenon appears to be generic for different actin lengths, which we controlled using gelsolin, an actin severing and capping protein. Figure 2b shows that for short actin rods, a similar de-condensation occurs as the D/A ratio is increased. A phase diagram summarizing the phase behavior of DNA-actin mixtures in the presence of spermidine for different actin lengths is shown in Fig. 2c.

The collective behavior of DNA and actin segments in the mixture is determined by a complicated balance between several effects. The presence of multivalent counterions affects the interactions between the similar and the dissimilar species (DNA-DNA, DNA-actin, actin-actin). Moreover, the entropy of mixing is expected to play a pivotal role like in any polymer mixture. To capture the essence of the phase behavior of the DNA-actin mixture, we consider a simple phenomenological Flory-Huggins theory for a mixture of polymers, rods, and the solvent. Let us assume that the polymers are of fixed length N and have a volume fraction of ϕ, the rods are of fixed length L and have a volume fraction of ψ, and naturally, the solvent occupies the rest of the volume with the corresponding fraction being $1-\phi-\psi$. The free energy associated with this mixture can be written as [16,17]

$$\begin{aligned} f \equiv \frac{Fa^3}{V\ k_{\rm B}T} \ &= \ \frac{\phi}{N}\ln\phi + \frac{\psi}{L}\ln\psi + (1-\phi-\psi)\ln(1-\phi-\psi) \\ &\quad +\chi_{\rm rp}\ \psi\phi + \chi_{\rm rs}\ \psi(1-\phi-\psi) + \chi_{\rm ps}\ \phi(1-\phi-\psi), \end{aligned} \tag{1}$$

where a is a monomer size, $k_{\rm B}T$ is the thermal energy, V is the volume of the sample, and the corresponding χ-parameters are defined in a manifest way. The above form for the interaction terms are only justified because the electrostatic correlation–induced attractions are short-ranged ([1]). Considering the experimental conditions chosen, the χ-parameters would have values such that the combinations rod-solvent (rs), and polymer-solvent (ps) would want to phase separate when alone.

To find the phase behavior of the system, we need to know the structure of the minima of the free energy function Eq. (1). For $\chi_{\rm rs}-\chi_{\rm rp}<\chi_{\rm ps}<\chi_{\rm rs}+\chi_{\rm rp}$, one finds that the function has three minima: $A:\ (\phi_A,\psi_A)=(0,0)$, $B:\ (\phi_B,\psi_B)=(\phi_s,\psi_l)$, and $C:\ (\phi_C,\psi_C)=(\phi_l,\psi_s)$, where $\phi_s\simeq e^{-N(\chi_{\rm rp}+\chi_{\rm rs}-\chi_{\rm ps})+1}$, $\psi_l\simeq 1-e^{-(1+2\chi_{\rm rs})+1/L}$, $\phi_l\simeq 1-e^{-(1+2\chi_{\rm ps})+1/N}$, $\psi_s\simeq e^{-L(\chi_{\rm rp}+\chi_{\rm ps}-\chi_{\rm rs})+1}$. Note that $l(s)$ corresponds to large (small). In the other parts of the parameter space, the number of minima changes to two; for $\chi_{\rm rs}+\chi_{\rm rp}<\chi_{\rm ps}$, A and C will be the minima (B disappears), and for $\chi_{\rm ps}<\chi_{\rm rs}-\chi_{\rm rp}$ there will be A and B left (C disappears). The minima have clear interpretations: A corresponds to the fully dilute phase, B corresponds to a polymer–poor rod–rich phase, and C corresponds to a polymer–rich rod–poor phase. The "–rich" domains would correspond to condensates, while the "–poor" domains would just mean the homogeneous phase.

The phase diagram can be determined by using the Maxwell construction. Because the values of ϕ_s and ψ_s are exponentially small, one can assume (to a reasonable approximation) that all the minima are sitting at the boundaries and thus the positions of the common tangent contact points needed for the binodal actually coincide with the minima. In the three-phase coexistence region corresponding to $\chi_{\rm rs}+\chi_{\rm rp}<\chi_{\rm ps}$, we can find the corresponding fractions of each phase in every point of the phase diagram by applying the lever rule to the two fields ϕ and ψ.

([1])A number of different mechanisms have been proposed for correlations leading to the attractive interactions observed in charged systems summarized in Ref. [1]. The shortest scale for the range of attractive interactions is a molecular one whilst the longest scale is given by half the Debye screening length of the solution. For our analysis, it is sufficient that the range of the attractive interaction is finite (i.e. much less than the system size).

Let us assume that we have a fraction x of phase B (corresponding to condensed actin), a fraction y of phase C (corresponding to condensed DNA), and a fraction $(1-x-y)$ of phase A. Also assume that we fix (experimentally) the average values for the two fields as $\bar{\phi}$ and $\bar{\psi}$. The lever rule then gives us $\bar{\phi} = x\ \phi_B + y\ \phi_C + (1-x-y)\ \phi_A$ and $\bar{\psi} = x\ \psi_B + y\ \psi_C + (1-x-y)\ \psi_A$, which can be solved to yield the two unknowns x and y as

$$x = \frac{\bar{\psi}\phi_l - \bar{\phi}\psi_s}{\psi_l\phi_l - \psi_s\phi_s}, \qquad y = \frac{\bar{\phi}\psi_l - \bar{\psi}\phi_s}{\psi_l\phi_l - \psi_s\phi_s}. \tag{2}$$

Let us now go back to the experimentally determined phase diagram of Fig. 2. Putting in numbers we find that the experiment was done at a fixed value of the actin volume fraction $\bar{\psi} = 0.005$, while the DNA volume fraction $\bar{\phi}$ was varied from 0.001 to 0.004, which corresponds to the window $0.2 < \bar{\phi}/\bar{\psi} < 0.8$. It appears that the majority of the phase diagram corresponds to the three-phase coexistence region where there are condensed DNA and condensed actin phases coexisting with each other as well as the dilute phase. As the ratio between the DNA concentration and the actin concentration $\bar{\phi}/\bar{\psi}$ is increased, Eq. (2) shows that the fraction of the actin condensate x is decreased. As shown in Fig. 2, the experiment reveals a transition to a state where the actin condensate fraction drops to zero at $(\bar{\phi}/\bar{\psi})_T \simeq 0.6$. One possible explanation for the observed transition is that it actually corresponds to the onset of vanishing of x as $\bar{\phi}/\bar{\psi}$ is increased. This would yield $(\bar{\phi}/\bar{\psi})_T = \phi_l/\psi_s$ [see Eq. (2)], which is considerably larger than one unlike the observed onset of 0.6. Moreover, the phase boundary would depend exponentially on L, while the observed phase boundary is actually independent of L.

Another possible explanation is that the χ-parameters actually depend on the DNA and actin concentration. For example, one can imagine that a competition between DNA and actin for counterion condensation would induce an effective interaction between the actin rods that depends on the density of DNA in the solution. The many-body nature of the correlation–induced attraction makes it possible that by changing the DNA concentration $\bar{\phi}$ the system crosses over from $\chi_{\rm rs}(\bar{\phi},\bar{\psi}) - \chi_{\rm rp}(\bar{\phi},\bar{\psi}) < \chi_{\rm ps}(\bar{\phi},\bar{\psi}) < \chi_{\rm rs}(\bar{\phi},\bar{\psi}) + \chi_{\rm rp}(\bar{\phi},\bar{\psi})$ corresponding to coexistence of condensed actin and condensed DNA to $\chi_{\rm rs}(\bar{\phi},\bar{\psi}) + \chi_{\rm rp}(\bar{\phi},\bar{\psi}) < \chi_{\rm ps}(\bar{\phi},\bar{\psi})$ that corresponds to uncondensed actin and condensed DNA solution. This would also be consistent with the observed independence of the phase boundary on the length of the actin rods L. Such an analysis is not appropriate for this letter and will be presented elsewhere [18].

A conclusive confirmation of the above picture would require a calculation of the χ-parameters based on the detailed physical considerations of the correlation–induced attraction in a mixture of actin and DNA, which may be a difficult task. Nevertheless, one could use order of magnitude estimates to check if the observed onset actually supports this picture. The close-packed DNA globules in the DNA-actin mixtures are likely to be fully charge compensated. If we assume that the DNA strands have a much greater affinity for the spermidine trivalent cations, we can estimate the concentration of spermidine remaining in solution after the condensation of DNA into globules. For 5 mM spermidine, and 3.8 mg/ml DNA (5.8 mM of base pairs), the effective spermidine concentration accessible to actin is ∼1.1 mM. We independently investigated the phase behavior of actin alone in the presence of spermidine, and find that the global concentration at the onset of actin condensation varies between 1 mM for short (∼3000 Å) filaments to 1.5 mM for long (∼10 μm) filaments [19]. This suggests that if DNA neutralization is assumed, the effective spermidine concentration accessible to actin is below the threshold required for actin condensation, in agreement with our observed results. We finally note that the effect of polydispersity in the length of the actin rods should also be taken into account for a full quantitative analysis of the experimental results.

In summary, the multivalent ion induced condensation in binary anionic polyelectrolyte mixtures exhibits a rich range of behavior. Mixtures consisting of DNA coils and F-actin rods

micro-phase separate into pure F-actin bundles and pure DNA toroids. Moreover, collective effects are important for the phase behavior of this system, and changes in the stoichiometry of the polyelectrolyte mixture can completely destabilize condensation of individual components.

* * *

It is our pleasure to acknowledge stimulating discussions with Peter Olmsted, Victor Bloomfield, and Bill Gelbart. This material is based upon work supported by the U.S. Department of Energy, Division of Materials Sciences under Award No. DEFG02-91ER45439, through the Frederick Seitz Materials Research Laboratory at the University of Illinois at Urbana-Champaign, and by the NSF DMR-0409369 and NIH 1R21DK68431-01.

REFERENCES

[1] W. M. Gelbart, R. F. Bruinsma, P. A. Pincus and V. A. Parsegian, *Physics Today*, **53** (2000) 38; Y. Levin, *Rep. Prog. Phys.*, **65** (2002) 1577; C. Holm, P. Kékicheff, R. Podgornik, *Electrostatic effects in soft matter and biophysics* (Kluwer Academic Publishers, Dordrecht) 2001.

[2] F. Oosawa, *Polyelectrolytes* (Marcel Dekker Inc., New York) 1971; B.-Y. Ha and A. J. Liu, *Phys. Rev. Lett.*, **79** (1997) 1289; A. P. Lyubartsev, J. X. Tang, P. A. Janmey and L. Nordenskiöld, *Phys. Rev. Lett.*, **81** (1998) 5465.

[3] I. Rouzina and V. A. Bloomfield, *J. Phys. Chem.*, **100** (1996) 9977; B. I. Shklovskii, *Phys. Rev. Lett.*, **82** (1999) 3268; N. Grønbech-Jensen, R. J. Mashl, R. F. Bruinsma and W. M Gelbart, *Phys. Rev. Lett.*, **78** (1997) 2477.

[4] G. S. Manning, *Q. Rev. Biophys.*, **2** (1978) 179.

[5] P. A. Pincus and S. A. Safran, *Europhys. Lett.*, **42** (1998) 103.

[6] R. R. Netz and H. Orland, *Eur. Phys. J. E*, **1** (2000) 203.

[7] R. Golestanian and T. B. Liverpool, *Phys. Rev. E*, **66** (2002) 051802.

[8] V. A. Bloomfield, *Curr. Opin. Struct. Biol.*, **6** (1996) 334; R. Podgornik, D. C. Rau and V. A. Parsegian , *Biophys. J.*, **66** (1994) 962; J. X. Tang and P. A. Janmey, *J. Biol. Chem.*, **271** (1996) 8556; T. E. Angelini, H. Liang, W. Wriggers and G. C. L. Wong, *Proc. Natl. Acad. Sci. USA*, **100** (2003) 8634.

[9] J. C. Butler *et al.*, *Phys. Rev. Lett.*, **91** (2003) 028301.

[10] G. S. Manning, *J. Chem. Phys.*, **51** (1969) 924; *J. Chem. Phys.*, **51** (1969) 934.

[11] C. A. Sheils, J. Kas, W. Travassos, P. G. Allen, P. A. Janmey, M. E. Wohl and T. P. Stossel, *Am. J. Pathol.*, **148** (1996) 919.

[12] At the present concentration range of DNA and spermidine, this is consistent with the observations of T. Iwataki, S. Kidoaki, T. Sakaue, K. Yoshikawa and S. S. Abramchuk, *J. Chem. Phys.*, **120** (2004) 4004.

[13] M. L. Henle and P. A. Pincus, *Cond. Matt.*, **2004** (0407645) .

[14] B.-Y. Ha and A. J. Liu, *Phys. Rev. Lett.*, **81** (1998) 1011; *Europhys. Lett.*, **46** (1999) 624.

[15] C. Huang and M. Olvera de la Cruz, *Macromolecules*, **35** (2002) 976.

[16] M. Rubinstein and R. Colby, *Polymer Physics* (Oxford University Press, New York) 2003.

[17] K. Bergfeldt, L. Piculell and P. Linse, *J. Phys. Chem.*, **100** (1996) 3680.

[18] O. V. Zribi, R. Golestanian, T. B. Liverpool and G. C. L. Wong, unpublished.

[19] The onset of condensation in actin is defined as the first appearance of the condensed lamellar network phase, which is a precursor to the condensed bundled phase. For more information, see: G. C. L. Wong, A. Lin, J. X. Tang, Y. Li, P. A. Janmey and C. R. Safinya, *Phys. Rev. Lett.*, **91** (2003) 018103.